Semicond. Sci. Technol. 10 (1995) 1494–1500. Printed in the UK

Change of minority carrier diffusion length in polycrystalline silicon by ultrasound treatment

S Ostapenko†, L Jastrzebski† and B Sopori‡

† University of South Florida, Center for Microelectronics Research, Tampa, FL 33620, USA
‡ National Renewable Energy Laboratory, Golden, CO 80401, USA

Received 17 May 1995, accepted for publication 20 July 1995

Abstract. We present a new approach for defect engineering by ultrasound treatment (UST) in solar-grade polycrystalline silicon wafers, leading to significant enhancement of minority carrier diffusion length (L) in wafer regions with short L. The maximum value of the UST effect is a 2.7 times increase of the diffusion length in regions of the sample with $L = 10$ to 25 μm. Using the surface photovoltage (SPV) method for non-contact mapping of the diffusion length, we have found both a positive and negative variation of L after UST in different wafer regions. The UST effect depends upon temperature, showing an activation energy of about 0.17 eV. A relaxation study of the UST effect shows two different behaviours: (i) stable result versus post-UST holding time, and (ii) partial or complete recovery of the diffusion length. Process (ii) is linked to the ultrasound-enhanced dissociation of FeB pairs followed by pairing kinetics.

1. Introduction

Ultrasound waves propagated through the bulk of a solid can affect the properties of point and extended defects [1]. This processing can be referred to as the process of ultrasound treatment (UST). It has been suggested that ultrasound vibrations applied to a semiconductor with a power density w, exceeding some threshold value, w_{th}, are able either to generate Frenkel pairs [2] or to force the dissociation of complex centres composed of two or more point defects [3]. The value of w_{th} was found to be of the order of 1–10 W cm^{-3} [2]. In the opposite case, i.e. when $w < w_{th}$, a different UST effect related to the interaction of point defects and extended lattice defects has been found in II–VI single crystals [4, 5] as well as in polycrystalline materials [6]. This effect of UST was interpreted as an enhancement of gettering by sinks (dislocations, grain boundaries, precipitates) of both intrinsic and extrinsic point defects. The ultrasound vibrations can reduce the energy barrier for the diffusion of point defects [7] as well as the barrier for their capture by sinks. The last mechanism, was confirmed as the ultrasound-stimulated reduction of the energy barrier allowing the EL2 centre in GaAs to undergo a metastable-to-stable transition [8]. UST was recently found to effect a dramatic improvement in the hydrogenation efficiency in polycrystalline silicon thin films (material for active matrix display thin-film transistors) [9]. In this study the ultrasound vibrations applied to hydrogenated films stimulated interface state passivation with atomic hydrogen. Therefore, it has been recognized that extended lattice defects such as dislocations, grain boundaries and precipitates may efficiently couple the energy of ultrasound vibrations with extrinsic and intrinsic point defects.

With the above in mind UST could be particularly important for processing in solar-grade polycrystalline silicon (poly-Si), which is one of key materials for solar cell applications [10]. The recombination properties of poly-Si are controlled by point defects (for example heavy metal impurities) and extended lattice defects (grain boundaries and dislocations) interacting with each other [11]. A critical parameters determining poly-Si quality is the minority carrier diffusion length which reflects the concentration of heavy metal impurities (Fe, Cu, Cr) dissolved in the crystal, as well as other crystallographic defects decorated by these impurities. It has recently been established that Cl and P gettering techniques are able to substantially increase the value of the diffusion length in poly-Si [11]. The improvement (increase) of the diffusion length was observed in wafer regions with a relatively high L value (100 to 260 μm), and was attributed to the gettering of dissolved heavy metals by Cl or P precipitates. A strong improvement in the diffusion length by P and Al gettering was also observed in low-quality polycrystalline Si [12]. Regions with a value of $L < 50$ μm, where crystallographic defects are the main recombination centres, were not affected by conventional gettering processes [11]. It is reported here that UST can be an alternative (or complementary) technique for the improvement of those regions with short diffusion lengths in solar-grade poly-Si.

0268-1242/95/111494+07$19.50

The non-contact method of surface photovoltage (SPV) mapping is a sensitive diagnostic technique for the measurement of the distribution of minority carrier diffusion lengths [13]. The SPV technique also provides a means for selective monitoring and quantitative measurement of the Fe concentration in p-type Si [14]. This has enabled us to reveal a link between the UST effect and Fe–B pair dissociation. According to this concept, poly-Si is considered a favourable material for the application of UST, while the SPV technique is suitable for monitoring changes in the diffusion length as stimulated by UST. In this paper we report such observations and explore different characteristics of the UST effect in comparison with ultrasound parameters. We also study the stability of the UST effect in relation to post-UST holding time and compare this relaxation behaviour with Fe–B pair association kinetics.

2. Samples and methods

Polycrystalline cast p-type Si wafers (B doped, 2–10 Ω cm) were studied. This material contains large single-crystalline grains with surface areas ranging from a few mm^2 to about 1 cm^2. Samples of thickness 0.5 mm were cut to 50×50 mm^2 squares from a poly-Si wafer to match the size of the piezoelectric transducer used as a source of ultrasound vibrations. The transducers had diameters of 23, 37 or 74 mm and thicknesses of 1.5 or 3 mm (PZT-5H ceramics covered by plain Cr/Au electrodes). The radial vibration mode at frequencies of f_r = 25, 48 or 80 kHz (the value of f_r is inversely proportional to the radius of a transducer) or thickness vibration modes at f_r = 590 and 1200 kHz were selected using an appropriate resonance frequency of the respective transducer. Transducers were driven by an a.c. voltage supplied from a function generator (HP 3312a) coupled with a wide-band power amplifier (ENI 240L). The samples subjected to UST were tightly bound by the back side to the surface of a transducer either with acoustic glue or by being pressed to the surface using a spring. By using this mounting, the front surface of a sample was practically free from any external mechanical contacts with the exception of a small spring spot of approximately 1 mm^2 and, therefore, was available for SPV mapping (figure 1). Each UST is specified by the set of following parameters:

(i) Amplitude of the acoustic strain generated by a transducer, $\varepsilon_{us} = 10^{-6}$–$10^{-5}$, which is proportional to the amplitude of the applied a.c. voltage. V_{us} = 4–40 V.

(ii) UST holding time, t_{us} = 10–60 min.

(iii) Temperature of the sample, T_{us} = 20–100 °C, which was measured *in situ* with an infrared pyrometer OS610, shown in figure 1.

(iv) Frequency or mode of ultrasound vibrations (radial or thickness). The resonance frequency of a transducer is a function of its temperature. For this reason, f_r had to be adjusted for every T_{us} to maintain acoustic resonance.

A commercially available, computer-controlled SPV system for the non-contact measurement of the minority carrier diffusion length, L, and corresponding lifetime, $\tau_n = L^2/D_n$ (D_n being the diffusion coefficient of electrons), was used for mapping of L before and after UST. In calculating τ_n, we used $D_n = 32$ cm^2 s^{-1}, which corresponds to a low doping limit. The technical details and principles of the SPV method have been published elsewhere [13]. In our study, the diffusion length was measured by a 177-point map or by a line scan of 10 to 15 points in the same sample before and after UST with varying parameters. Since cast poly-Si is a strongly inhomogeneous, special precautions were taken to exactly compare the same wafer regions before and after UST. The reproducibility of the sample positioning was 0.5 mm while the accuracy of the L measurements was better than 1% for an SPV signal amplitude of 1 mV. The 2 mm diameter SPV probe sets a limit for spatial resolution in our study. Iron concentration maps and profiles were determined using the optical Fe–B pair disssociation method combined with the measurement of L as discussed in [14].

3. Experimental results

Two line scans of diffusion length before (L_{ref}) and after the sample was subjected to UST (L_{ust}) are shown in figure 2. The increase of L is observed in this sample after UST with the following parameters: $V_{us} = 5$ V, $t_{us} = 30$ min, $T_{us} = 55$ °C and $f = 80$ kHz. The strongest UST effect (a 2.7 times increase of L which corresponds to a more than 7 times increase of lifetime) is found in the region with the shortest diffusion lengths, L = 10–15 μm. The increase of L reaches 12–40% for the sample region with larger L.

By mapping the entire wafer, we found that the effect of UST can be significantly different for various regions of the sample. This result is consistent with the strong inhomogeneity of recombination parameters in solar-grade poly-Si [11], in particular the variation of diffusion length as presented in figure 3(a). In figure 3, the line scans of diffusion length for the same part of sample are shown: (a) as L distribution prior to UST; (b) the change of diffusion length by UST in terms of the quantity $\Delta L/L = (L_{ust} - L_{ref})/L_{ref}$; and ($c$) as a post-UST relaxation of $\Delta L/L$. Three consecutive UST treatments were applied to a sample and specified by the following sets of parameters: UST1: $V_{us} = 40$ V, $t_{us} = 30$ min, $T_{us} = 40$ °C, $f = 48$ kHz; UST2: 55 V, 30 min, 50 °C, 48 kHz; UST3: 32 V, 80 min, 50 °C, 48 kHz. The sign of ΔL is different in various regions of a sample. Positive variations of L are observed for the regions with the shortest diffusion length while negative values of ΔL are found in regions with relatively large $L > 25$ μm.

The value of $\Delta L/L$ versus L_{ref} for the entire 177-point map is shown in figure 4. The area within the full curves represents data measured immediately after UST, while the broken curves represent the limits of $\Delta L/L$ after post-UST relaxation. The values of $\Delta L/L$ range from −25% to 58% which is typical for different poly-Si samples subjected to UST. Again, we emphasize that the region with the shortest diffusion length, L = 7.5–15 μm, demonstrates the strongest increase of L.

The change of the diffusion length is a function of UST parameters and depends upon the UST temperature,

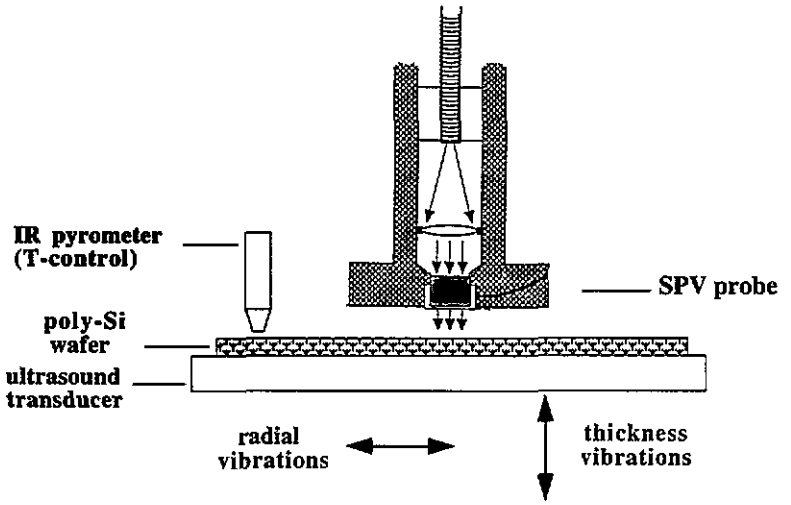

Figure 1. A schematic diagram of the ultrasound treatment of poly-Si solar-grade material using an external ultrasound transducer. Two vibration modes (radial and thickness) used in UST experiments are shown. A non-contact surface photovoltage technique is used to monitor diffusion length changes due to UST.

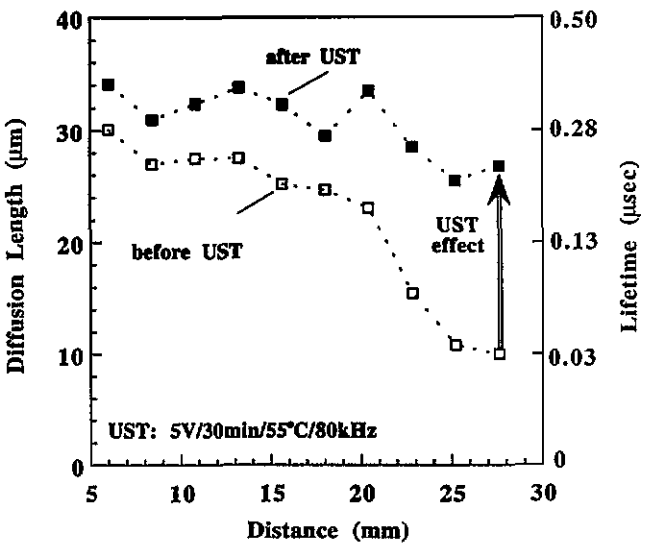

Figure 2. Line scans of diffusion length in a sample before and immediately after UST with the specified parameters.

as shown in figure 5. The reference data point (L_{ref} = 10.5 μm) shows the value of L before UST. The increase of T_{us} above 35 °C results in an enhancement of the UST effect; however, at T_{us} higher than 64 °C, a decrease of L with respect to its maximum value occurs.

The change of diffusion length versus UST holding time, t_{us}, expressed as the quantity $\Delta L^{-2} = L_{ref}^{-2} - L_{ust}^{-2}$, which is proportional to the change of concentration of recombination centres, can be approximated by a first-order kinetic

$$\Delta L^{-2} = \Delta L_{max}^{-2}[1 - \exp(-t_{us}/\tau)] \qquad (1)$$

where ΔL_{max}^{-2} is the maximum value of the UST effect achieved at long treatment times. The characteristic time of the UST process, τ, is 20 min at 40 °C. We estimated the UST activation energy as $\varepsilon_{ust} = 0.17 \pm 0.05$ eV using the Arrhenius plot of $\ln \tau$ versus T_{us}^{-1} as shown in figure 6. The data points represent the value of τ measured in different poly-Si samples by averaging L from particular regions of the SPV map which demonstrated the strongest UST effect.

An important issue is the stability of the UST effect versus post-UST holding time. Two different post-UST behaviours of ΔL specific to particular sample areas are observed (figure 3(*c*)). The first is a stable positive change of L which did not show any noticeable relaxation for seven days at room temperature or after the annealing of the sample for 1 h at 80 °C. This behaviour characterizes the regions with the shortest L (L = 7–15 μm) and the maximum $\Delta L/L$ as shown in figure 4 (area within the dashed lines). The second behaviour is partial or complete relaxation of ΔL to a new stable value after the sample was stored for 5–10 h at room temperature. The relaxation either compensates for the effect of UST, i.e. had ΔL of the opposite sign, or enhances the UST change of L as depicted in figure 3(*c*). In the general case, a superposition of stable and unstable UST effects occurs.

The kinetics of UST relaxation shows a characteristic time of 14 min at 75 °C (figure 7). We compared this relaxation curve with the kinetics of Fe and B pairing (see the following discussion) which were performed after Fe–B optical dissociation in the same region of a sample measured in both cases. The characteristic Fe–B pairing time after optical dissociation was determined as 2 min at 75 °C which is consistent with published data in Cz-Si [14]. These experiments provide a background for the UST model now to be discussed.

4. Discussion

The diffusion length and bulk lifetime, τ_n, of electrons in p-type Si can be expressed versus the diffusion coefficient of electrons, D_n, their thermal velocity, v_{th}, as well as the capture cross section and concentration of recombination

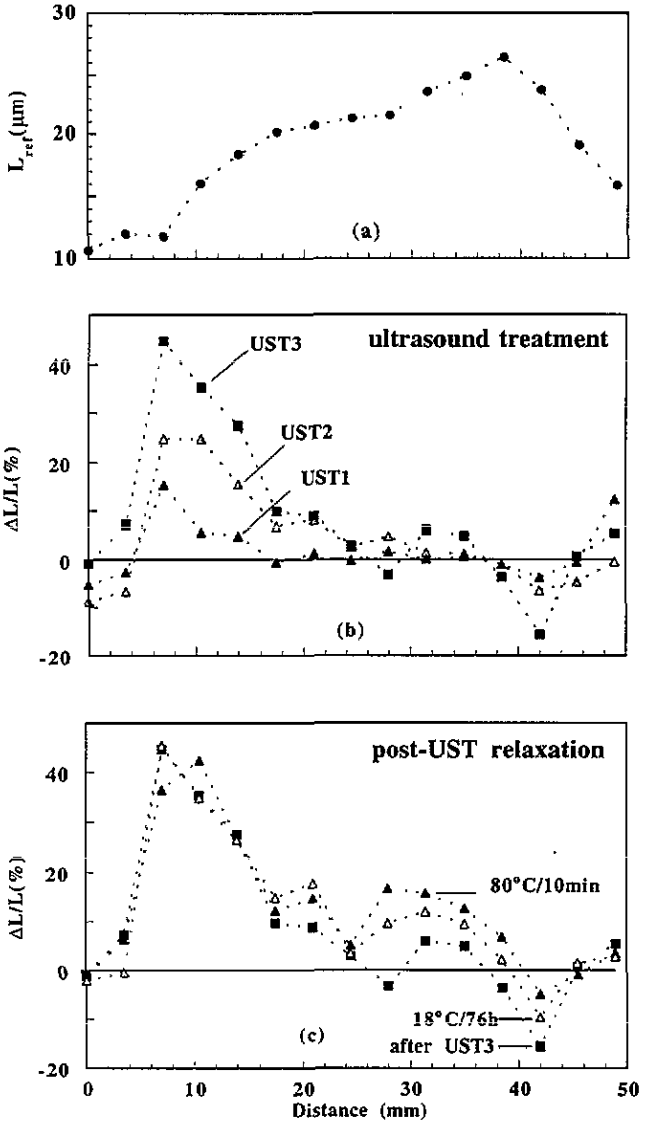

Figure 3. (*a*) Distribution of diffusion length in a poly-Si sample before UST. (*b*) Line scans of the relative variation of L after three consecutive UST treatments. (*c*) Post-UST relaxation of $\Delta L/L$ at room temperature (76 h) and 80 °C (10 min). The regions with stable and unstable UST effects are shown.

centres, σ_{ni} and N_i, as follows

$$L^{-2} = (D_n \tau_n)^{-1} = D_n^{-1} v_{th} \sum \sigma_{ni} N_i. \qquad (2)$$

Therefore, changes in the diffusion length of poly-Si wafers stimulated by UST can result from the variation of σ_{ni} and/or N_i, assuming that the diffusion coefficient of minority carriers it not varied after treatment.

The identification of different recombination processes in solar-grade poly-Si which contribute to the value of L is not adequate at present to provide a quantitative separation of contributions from precipitates, dislocations, grain boundaries and point defects. Within the framework of this study, we were only able to separate in the UST effect the role of Fe impurities, a typical contamination in silicon [15]. Dissolved interstitial Fe in boron-doped p-type Si tends to form Fe_i–B_s pairs which are stable at room temperature. These pairs can be dissociated either by thermal annealing at 200 °C followed by quenching of a sample to room temperature [16] or by using

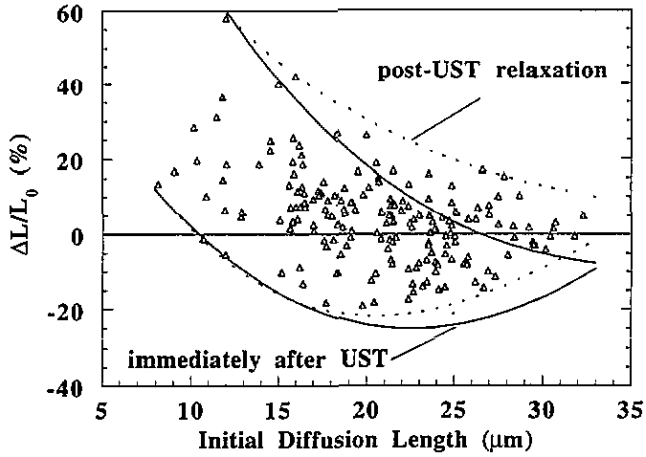

Figure 4. Relative variation of the diffusion length versus absolute value of L for a 177-point map immediately after UST (area within the full curves) and after post-UST relaxation (area within the broken curves). The points represent the relaxed state of the diffusion length. The increase of L for a short diffusion length (less than 15 μm) is demonstrated.

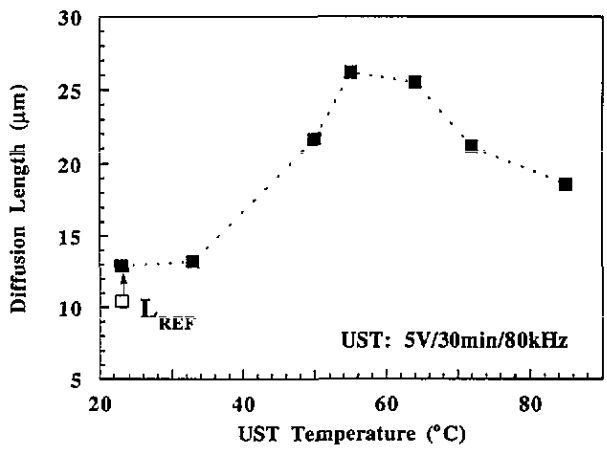

Figure 5. Temperature dependence of the UST effect. The initial value of diffusion length is $L_0 = 10.5$ μm.

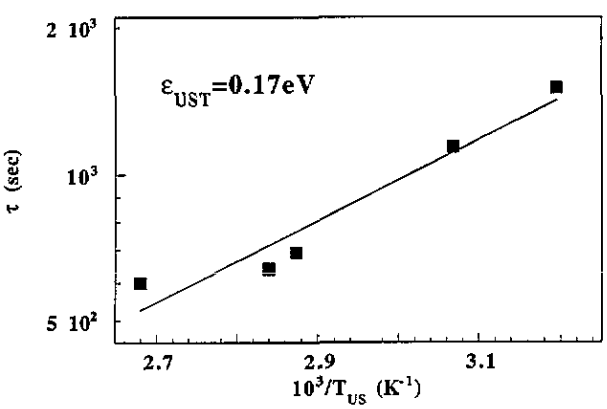

Figure 6. Arrhenius plot of UST rate evaluated from equation (1) versus UST temperature.

enhanced dissociation processes, for example minority carrier injection [17] or light illumination [14]. The variation of a minority carrier lifetime under UST has been previously observed in Cz-Si containing so-called 'ring defects' [18]. A process of enhanced Fe–B pair

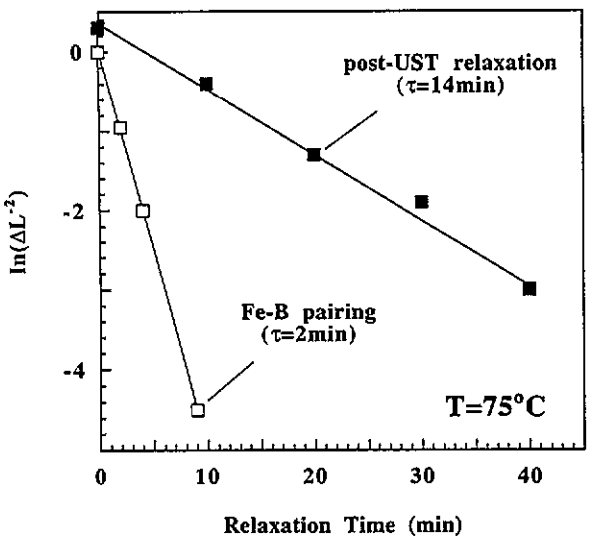

Figure 7. Relaxation of the diffusion length at 75 °C due to the Fe–B pairing process measured after Fe–B pair optical dissociation at room temperature (open points) and after UST (full points) measured in the same region of a poly-Si wafer.

dissociation was suggested as an initial step of UST. We found experimental evidence supporting the fact that the UST effect in poly-Si regions which show relaxation behaviour can be attributed to ultrasound-enhanced Fe–B dissociation.

By using the optical dissociation method [14], we determined the concentration of Fe–B pairs in our samples. This method is based on an increase of the electron recombination capture cross section (and, consequently, decrease of L), when Fe–B pairs are transformed to isolate Fe_i. Calculations were carried out using the equation [16]

$$[\mathrm{FeB}] = 1.05 \times 10^{16}(L_1^{-2} - L_0^{-2}) \qquad (3)$$

where L_0 and L_1 are the respective diffusion lengths before and after Fe–B pair dissociation. We measured the concentration of Fe–B pairs in our samples to be in the range of 10^{12} to 10^{13} cm^{-3}. If one assumes that the UST effect is the result of Fe–B pair dissociation, it can be estimated, by using equation (3), that for $L_{ref} = 20$ μm and $\Delta L/L = -25\%$ as observed in the UST experiment that the required change in Fe–B pair concentration would be about 5×10^{12} cm^{-3} which is within the limits of available Fe–B pair concentration in our samples.

The ultrasound enhancement of Fe–B pair dissociation was recently discovered in p-type Cz-Si intentionally doped with Fe [19]. By comparing the rate constants of Fe and B pairing kinetics, and the post-UST relaxation of the diffusion length, it was unambiguously demonstrated that UST provides a breaking of Fe–B pairs. In the case of poly-Si, the following experimental facts support the hypothesis that Fe–B pairs can also participate in the UST process:

(i) The effect of UST is strongly suppressed when the crystal is illuminated by halogen lamp light (10 mW cm^{-2}) at room temperature initially or during UST, which according to [14] forces the enhanced dissociation of Fe–B pairs. These results are presented in table 1 where the changes in L for the same sample treated by ultrasound at different states of Fe are presented. It is clear that the UST applied to a sample with paired Fe and B (before illumination) decreases L, while UST (with the same parameters) applied to this sample after Fe–B dissociation shows conventional pairing kinetics (increase of L). We noticed, however, that the Fe–B pairing rate after UST and optical pair dissociation is significantly different as shown in figure 7. This problem is discussed below.

(ii) A UST activation energy of 0.17 ± 0.05 eV is close to the activation energy for Fe–B pair optical dissociation (0.25 eV) [20] which means that the thermal barrier to break the pair is suppressed in both cases. We believe, however, that a different mechanism is responsible for Fe–B pair dissociation in the case of UST. It has been established that anisotropic complexes of point defects, for example, donor–acceptor pairs, can be reoriented when the acoustic vibrations are applied to a crystal. This mechanism is well documented, for instance, in the case of Li_i–B_s pair reorientation in silicon [21]. Such an ultrasound-enhanced reorientation process may well stimulate the breaking of Fe–B pair coupling due to the fact that to move from the one nearest neighbour interstitial position to the equivalent one the Fe_i has to 'jump' to the next nearest interstitial from the substitutional boron atom; the binding of the Fe–B pair components thus becomes weaker due to an increase in the interpair distance [21]. The reduced activation energy of the UST process (figure 6), in comparison with the Fe–B thermal dissociation energy of 0.65 eV in Si single crystals [16], can be interpreted as a lowering of the Fe–B binding energy.

(iii) The relaxation of the UST effect occurs in a similar temperature range as the pairing process of dissociated Fe–B pairs. The pairing of Fe and B after optical dissociation in a sample with resistivity of 2 Ω cm shows a time constant of 2 min at 75 °C which is consistent with the data for Cz-Si [14]. An important result is the observed difference in the kinetic rate for the UST effect relaxation and Fe–B association kinetics (figure 7). This may be interpreted in terms of the capture of released Fe_i by sinks. If captured by Fe_i atoms are unstable at room temperature (for example due to a small binding energy), they can be thermally released from sinks and repaired with boron, therefore demonstrating similar behaviour to the well-documented pairing kinetics of Fe_i and B_s. The trapping of Fe_i by sinks can significantly change the rate of pairing kinetics if the release of Fe from a sink is a rate-limiting process for Fe and B association. This accounts for a longer UST relaxation time versus characteristic time of Fe–B pairing in poly-Si as opposed to Cz-Si wafers [19].

Summarizing the UST effect with regards to Fe–B pairs, we assert that the ultrasound-enhanced dissociation of Fe–B pairs is a possible process contributing to the post-UST relaxation of diffusion length in poly-Si. The complete UST mechanism is a two-step process. In the first step, ultrasound vibrations enhance the dissociation of Fe–B pairs. This process shows a similar activation energy for different regions of a wafer as well as in various samples. In the second step, the released Fe_i^+ are captured at sinks. If captured Fe_i^+ ions form electrically inactive

Table 1. Fe-related effects contributing to the effect of ultrasound treatment on diffusion length in poly-Si.

State of Fe	Diffusion length before UST (μm)	Diffusion length after UST (μm)	Relevant mechanism
Fe_i–B pair [a]	27	22	UST-enhanced pair dissociation
Fe_i [b]	21	26	Thermal pairing of Fe and B

[a] After annealing for 10 min at 80 °C in the dark.

[b] After optical dissociation for 10 s at room temperature (10 mW cm^{-2}).

recombination centres, then the UST increases the diffusion length ($\Delta L > 0$) due to a decrease of N, as was suggested in [22]. On the other hand, if the released Fe_i ions form centres with capture cross sections larger than for Fe–B pairs, a negative change of ΔL will be observed [23].

In sample regions with relatively short diffusion lengths, L = 10–15 μm, showing a positive change of L (figure 2), which is stable versus post-UST time, the concentration of Fe–B pairs is too low to account for an observed UST effect. By using equation (3) with parameters $L_0 = 10$ μm and $L_1 = 27$ μm (figure 2), we obtain Δ[FeB] = 8×10^{13} cm^3 which is approximately one order of magnitude higher than the maximum concentration of Fe–B pairs in our samples. Therefore we may assume that the recombination characteristics of crystallographic defects such as dislocations, grain boundaries and precipitates contribute to the regions of short diffusion length [11] and can also be affected by UST. It is recognized that a dislocation network in poly-Si solar-grade material can be an effective place for impurity precipitation, in particular for Fe precipitates [23]. This process of extended defect decoration by impurities can bring about a reduction of diffusion length by introducing effective recombination levels for minority carriers, especially in regions of short diffusion length [11]. We can speculate, based on our study, that such crystallographic defects decorated by impurities can also be subjected to UST. In fact, dislocations can effectively absorb the ultrasound vibrations by the mechanism of Granato and Lucke [24]. A dislocation line vibrating in the ultrasonic field is able to generate an alternating strain field which provides a driving force to dissolve a decorated impurity atmosphere around a dislocation. This would lead to an increase of diffusion length in the relevant sample regions. Further experiments are necessary to establish the validity of the suggested process.

A stable or unstable UST effect can dominate in different regions of a wafer and can account for the link of changes in ΔL to a particular sample area. Moreover, both processes may superimpose, which would result in the observed maximum of UST temperature dependence (figure 5). In fact, thermal association of Fe_i (released from sinks) and B is activated with elevated temperature. Therefore, at higher T_{us} pairing kinetics cancel the process of unstable UST while the second mechanism, stable versus post-UST time, dominates in the change of the diffusion length.

In conclusion, we observed and explored the effect of ultrasound-enhanced changes of diffusion length in solar-grade polycrystalline silicon. An increase of diffusion length which is stable versus post-UST holding time is observed in wafer regions with the shortest $L < 15$ μm where crystallographic defects decorated by impurities are probably affected by the ultrasound vibrations. Based on this result, we assert that ultrasound treatment offers an effective means for defect engineering in poly-Si. We have shown in our study that ultrasound-enhanced Fe–B pair dissociation, and the subsequent thermal association of Fe_i and B, are relevant processes contributing to the unstable part of the UST effect.

Acknowledgment

The authors would like to thank Professor J Lagowski for helpful discussions and critical comments. We also acknowledge Dr J Kalejs of Mobil Solar Energy Corporation, Dr Frederick Schmid of Crystal Systems and Dr P Stalhofer of Wacker-Chemie for providing the polycrystalline wafers. This work was supported by a grant from the NREL.

References

[1] de Batist R 1972 *Internal Friction of Structural Defects in Crystalline Solids* (Amsterdam: North-Holland) pp 111, 210

[2] Ostrovskii I V and Lisenko V N 1982 *Sov. Phys.–Solid State* **24** 682

[3] Gromashevskii V L, Dyakin V V, Sal'kov E A, Sklyarov S M and Khilimova N S 1984 *Ukr. Fiz. Zh.* **29** 550

[4] Zdebskii A P, Mironyuk N V, Ostapenko S S, Savchuk A U and Sheinkman M K 1986 *Sov. Phys.–Semicond.* **20** 1167

[5] Garyagdyev G, Gorodetskii I Ya, Dzhumaev B R, Korsunskaya N E, Rarenko I M and Sheinkman M K 1991 *Sov. Phys.–Semicond.* **25** 248

[6] Zdebskii A P, Mironyuk N V, Ostapenko S S, Khanat L N and Garyagdyev G 1987 *Sov. Phys.–Semicond.* **21** 570

[7] Krevchik V D, Muminov R A and Yafasov A Ya 1981 *Phys. Status Solidi* a **63** K159

[8] Buyanova I A, Ostapenko S S, Sheinkman M K and Murrikov M 1994 *Semicond. Sci. Technol.* **9** 158

[9] Ostapenko S, Henley W, Karimpanakkkel S, Jastrzebski L and Lagowski J 1994 *Int. Display Research Conf. (Monterey, CA)* (Santa Ana, CA: Society for Information Display) p 299

[10] Watanabe H 1993 *MRS Bull.* October 29

[11] Jastrzebski L, Henley W, Schielein D and Lagowski J 1994 *12th NREL Photovoltaic program Review (A/P Conf. Proc. 306)* ed R Noufi and H S Ullal (New York: American Institute of Physics) p 498
[12] Loghmarti M, Stuck R, Muller J C, Sayah D and Siffert P 1993 *Appl. Phys. Lett.* **62** 979
[13] Lagowski J, Edelman P, Dexter M and Henley W 1992 *Semicond. Sci. Technol.* **7** A185
[14] Lagowski J, Edelman P, Kontkiewicz A M, Milic O, Henley W, Dexter M and Jastrzebski L 1993 *Appl. Phys. Lett.* **63** 3043
[15] Jastrzebski L, Milic O, Dexter M, Lagowski J, DeBush R, Nauka K, Gordon M and Persson E 1993 *J. Electrochem. Soc.* **140** 1152
[16] Zoth G and Bergholz W 1990 *J. Appl. Phys.* **67** 676
[17] Kimerling L C and Benton B S 1982 *Physica* **116B** 297
[18] Ostapenko S S, Ikeda N and Shimura F 1994 *Semiconductor Silicon* ed H R Huff *et al* (Pennington, NJ: Electrochemical Society) p 856
[19] Ostapenko S and Bell R 1995 *J. Appl. Phys.* **77** 5458
[20] Lagowski J, Kontkiewicz A M, Henley W, Dexter M, Jastrzebski L and Edelman P 1994 *Defect Recognition and Image Processing in Semiconductors and Devices (Inst. Phys. Conf. Ser. 135)* ed J Jimenez (Bristol: Institute of Physics) p 271
[21] Novick A S and Berry B S 1972 *Anelastic Relaxation in Crystalline Solids* (New York: Academic) p 324
[22] Wunstel K and Wagner P 1982 *Appl. Phys.* A **27** 207
[23] Bailey J and Weber E R 1993 *Phys. Status Solidi* a **137** 515
[24] Granato A V and Lucke K 1966 *Physical Acoustics* vol 4A, ed W P Mason (New York: Academic) p 225